Article

Chinese Science Bulletin

Environmental Science & Technology

October 2013 Vol.58 No.30: 3715–3720

doi: 10.1007/s11434-013-6040-7

Effect of microstructure and surface chemistry in liquid-phase adsorptive nicotine by almond-shell-based activated carbon

YANG JiLiang, FANG Fang & ZHOU JianBin*

College of Chemical Engineering, Nanjing Forestry University, Nanjing 210037, China

Received March 19, 2013; accepted July 10, 2013

The effect of microstructure and surface chemistry on nicotine adsorption capacity of almond-shell-based activated carbon was studied. Almond-shell-based activated carbon was reactivated or modified with steam, $ZnCl_2$ and $NaHSO_4$ separately. The surface area and pore structure parameters of activated carbon were determined from the adsorption-desorption isotherm of nitrogen at 77 K. Boehm titration and FTIR were explored to determine the surface oxygen groups. The results revealed that nicotine adsorption from solution on carbons depend on the micropores and phenolic groups. A strong correlation between the amounts of adsorbed nicotine and the phenolic groups was observed, whereas the higher amounts of carboxylic groups decrease the nicotine adsorption capacity on activated carbons.

activated carbon, nicotine adsorption, microstructure, surface chemistry

Citation: Yang J L, Fang F, Zhou J B. Effect of microstructure and surface chemistry in liquid-phase adsorptive nicotine by almond-shell-based activated carbon. Chin Sci Bull, 2013, 58: 3715–3720, doi: 10.1007/s11434-013-6040-7

Nicotine which appears in mainstream cigarette smoke is a high-toxic agent in large quantity [1,2]. However, cigarette production generates large quantity of waste water with nicotine, which can easily pollute groundwater and affect human health. Some studies were performed with solid adsorbents to determine the adsorption capacity [3,4] with activated carbon as a reference adsorbent, but the application of modified activated carbon (changes of microstructure and surface oxygen groups) into adsorption of nicotine from aqueous solution has not been systematically investigated and reported.

Our previous work shows that micropores and the surface chemistry of activated carbons play important roles during adsorption [5], and in this study, the aim is to determine which oxygen surface group plays a decisive role. Reactivation with steam and $ZnCl_2$ were employed for changing the microstructure and surface chemistry of almond-shell-based activated carbon, and a new chemical modification method was also used for changing the surface chemistry. $NaHSO_4$ solution is a good oxidation agent because its acidity is weaker than HNO_3 and could not destroy the microstructure of activated carbon. Moreover, Na^+ can be adsorbed onto the surface of activated carbon and create some micropores during the heat process due to the escape of Na atom. In the present work, we focus on examining the effects of microstructure and the type of surface oxygen groups on the adsorption performance.

1 Experimental

1.1 Reagents

Nicotine ($C_{10}H_{14}N_2$) was purchased from Langze, Nanjing (99% purity). Nicotine solutions (50, 100, 150, 200, 250, 350, 500, 600 and 750 mg/L) were prepared. All chemicals were at analytical grade and used without further purification. Double deionized water (R20 Unique 18.20 MΩ cm conductivity) was used for all solutions.

1.2 Reactivation/modification of almond shell-based activated carbon

The almond shell-based activated carbon was obtained from

*Corresponding author (email: zjb527@gmail.com; zhoujianbin@njfu.com.cn)

Huajing, Chengde, and was regularly used for removing organics from industrial wastewater. Before use, the activated carbon was sieved to the particle size of 180–200 mesh and named AC. The steam reactivation sample was prepared as follows: 400 g of AC was placed into an iron tube furnace and activated at 1073 K for 2.5 h under a water vapor flow of 7 mL/min, which was provided by injecting liquid water to a hot reactor through a peristaltic pump. After activation, the sample was cooled in water and washed with 0.1 mol/L HCl at 368 K for 30 min. Then warm water (333 K) was used to remove the excessive iron ions from the equipment until the washings reached about pH 7, followed by drying in an oven at 343 K for 16 h. This activated carbon was named AC-H. The $ZnCl_2$ reactivation sample was prepared as follows: 10 g of AC was added into 100 mL of $ZnCl_2$ (30% *w*/*t*), stirred for 2 h and then dried in the stove. The mixture was placed in an iron capsule and activated at 773 K in a furnace for 1 h. The temperature was raised from room temperature to 773 K at 5 K/min. Then the sample was washed with 0.1 mol/L HCl at 368 K for 30 min and then warm water at 333 K was used to remove the excessive Zinc ions until the washings reached about pH 7, followed by drying in an oven at 343 K for 16 h. This activated carbon was named AC-Z. The $NaHSO_4$-modified activated carbon was prepared as follows: 10 g of AC was added into 100 mL of $NaHSO_4$ (25% *w*/*t*), stirred for 2 h, and then dried in the stove at 373 K for 12 h. The mixture was placed in an iron capsule and activated at 573 K in the tube furnace for 2 h under nitrogen atmosphere at a flow rate of 200 mL/min. The temperature was raised from room temperature to 573 K at 5 K/min. The modified activated carbon was washed with hot water until the washings reached about pH 7, and was finally dried in the oven at 343 K for 16 h. The modified activated carbon was named AC-N.

1.3 Characterization of activated carbon

The surface area and pore structure parameters of activated carbon were determined from the adsorption-desorption isotherm of nitrogen at 77 K using a Surface Area and Porosity Analyzer (Quantachrome Corporation, USA). The samples were degassed at 423 K for 24 h before measurement. The surface area and micropore volume were determined by BET method and t-plot method, respectively.

The surface oxygen groups were determined by Boehm titration. The four 0.25-g carbon samples were each placed in a 150 mL Erlenmeyer flask and added with 25 mL of 0.1 mol/L NaOH, Na_2CO_3, $NaHCO_3$ and HCl, respectively. The flasks were sealed and shaken for 24 h. After the mixtures were filtered, the filtrates were titrated by 0.1 mol/L NaOH or HCl [6,7].

Fourier transform infrared spectroscopy (FTIR) (Nicolet 380, Thermo, USA) was used to determine the vibration frequency variations of the functional groups in AC, AC-H, AC-Z and AC-N.

1.4 Adsorption experiments

Batch equilibrium adsorption experiments were conducted as follows: 50 mg of activated carbon was placed in contact with 50 mL of nicotine solution in a sealed Erlenmeyer flask and the mixture was shaken at 100 r/min. The initial concentrations of nicotine were 50, 100, 150, 250, 350, 500, 600 and 750 mg/L, and the adsorbed amount of nicotine was investigated at different temperatures (298, 308 and 318 K). After adsorption, the adsorbent was filtered from the samples, and the nicotine content in each filtrate was determined by Reversed Phase High-Performance Liquid Chromatography (RP-HPLC). The conditions for RP-HPLC were: Angilent Zorbax C_{18} column (4.6 mm×250 mm, 5 μm), temperature of 308 K, methanol (A)/2.5% *w*/*v* acetic acid buffer (B) (A:B=3:2, *v*/*v*) as the mobile phase at 1 mL/min, UV wavelength at 259 nm, and injection volume of 10 μm. The HPLC chromatogram under these conditions shows that nicotine was determined selectively with high sensitivity, and the chromatographic peak is sharp without distinct asymmetry. Because the concentrations of nicotine were low and the whole adsorption process was carried out in sealed Erlenmeyer flasks, the nicotine loss caused by heating was ignored. The adsorbed amount of nicotine (q, mg/g) was calculated by mass balance as follows:

$$q = \frac{C_0 - C_i}{m} \times v, \quad (1)$$

where C_0 and C_i are the initial and final concentrations (mg/L), v is the volume (L) of solution and m is the mass of activated carbon (g).

2 Results and discussion

2.1 Characterization of porous texture

The adsorption isotherms of nitrogen at 77 K for AC, AC-H, AC-Z and AC-N are shown in Figure 1. The isotherms of all the activated carbons show typical Type-I features that indicate microporous materials are in a narrow pore size distribution [8]. The slopes of curves gradually increase and the isotherms exhibit a hysteresis loop near a relative pressure of 0.4 in the desorption branches, indicating that the materials have some large micropores or mespores [9]. The surface areas were calculated by BET, and the pore volumes for mesopores and micropores were calculated by BJH and t-plot, respectively. The BET surface areas, average pore widths, micropore volumes and total pore volumes are listed in Table 1. It can be seen that the three treatment methods do not show obvious differences in surface areas, whereas the porous structures changed more significantly. For all reactivation or modification treatments, these samples developed micropore structure, especially AC-N. That is because Na^+ in the $NaHSO_4$ solution can be adsorbed onto the surface of activated carbon and create some micropores

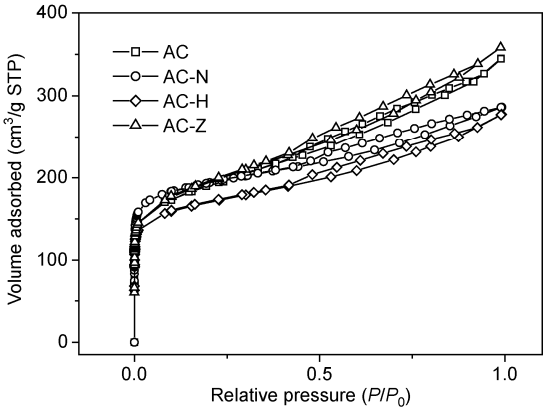

Figure 1 Nitrogen adsorption/desorption isotherm at 77 K on activated carbons.

Table 1 Textural parameters of activated carbons

Characterization	AC	AC-H	AC-Z	AC-N
BET surface area A (m^2/g)	685	630	697	731
Average pore width d (nm)	3.13	2.73	3.18	2.43
Micropore volume v_{micro} (cm^3/g)	0.12	0.17	0.14	0.22
Total pore volume v_T (cm^3/g)	0.54	0.43	0.55	0.44
v_{micro}/v_T w (%)	22.2	39.5	25.5	50.0

during heating due to the escape of Na atom. On the other hand, the acidic of the $NaHSO_4$ solution leads to the destruction of some original porous structures and to slightly higher external surface area and micropore volume [10]. AC-Z has larger pores than AC-H and AC-N, indicating that activation of $ZnCl_2$ is favorable to generation of larger mesopores. For AC-H, high temperature treatment could lead to the collapse of mesopore and the opening of some closed pores [11]. Therefore, the total pore volume of AC-Z increases while that of AC-H decreases.

The micropore size distributions are shown in Figure 2. It clearly shows that AC-H is in the similar micropore size distribution as AC-Z. Their micropores are concentrated around 0.5 and 1.1 nm, respectively, while the micropores of AC and AC-N are concentrated around 0.55 and 0.8 nm, respectively.

2.2 FTIR and Boehm titration data

The FTIR spectra (Figure 3) present the vibration frequency changes of the functional groups in the activated carbons. Strong adsorption peaks occur at 3500–3300, 1740–1480 and 1300–1000 cm^{-1}, and weak adsorption peaks occur at 2376, 2340, 544 and 448 cm^{-1}.

The broad band at 3500–3300 cm^{-1} is assigned to hydroxyl group or adsorbed water [12], and the bands at 1460–1350 and 480–460 cm^{-1} can be assigned to the stretching vibrations of aliphatic C–H [11]. The absorption band at 2400–2300 cm^{-1} can be attributed to CO_2. The band at 1740–1480 cm^{-1} is assigned to the stretching vibrations of C=O in carboxylic acids, anhydrides, lactones, esters, carboxylic salts, carboxylo-carbonates, quinones, and hydroxyquinones [13,14], and C=C in carboxylic or pyridine-like structure [15]. A intense band at about 1300–1000 cm^{-1} corresponds to the stretching in C–O, C–O–C, O–H in carboxylic acids, anhydrides, lactones, esters, ethers, phenols, epoxides and carboxyl-carbonates, which are also overlapped [11–16].

The adsorption band in Figure 3 exhibits the presence of surface oxygen groups O–H, C–H, CO_2, C=O and C–O or C–O–C in the FTIR spectrum of activated carbons. The clear differences among the four samples were showed in the adsorption band at 1740–1480 and 1300–1000 cm^{-1}. Compared with AC, the adsorption peaks at 1220 and 1090 cm^{-1} were shifted to around 1105 and 1028 cm^{-1}, respectively. The band at 1700–1500 cm^{-1} can be attributed to surface carbonyl, quinones and ketone, and the band at 1090 cm^{-1} can be attributed to ethers. These results indicate that the heat treatment at 1073 K led to the decomposition of surface carbonyl and quinone groups. The same results were found by Shangguan et al. [11]. On the other hand, there were new surface oxygen groups C=O and C–O or C–O–C generated in AC-Z during the heat treatment due to the

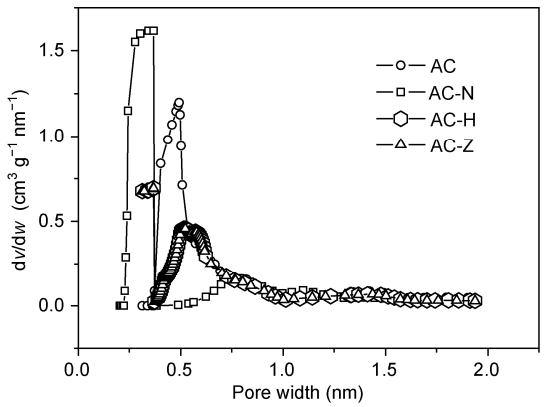

Figure 2 Micropore size distributions of activated carbons

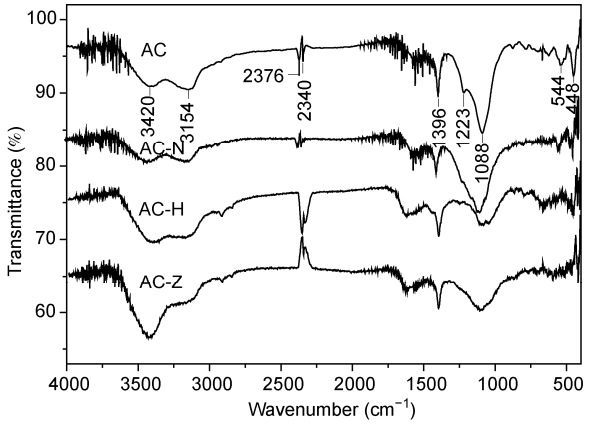

Figure 3 FTIR spectra of activated carbons.

activation of $ZnCl_2$.

The results of the Boehm measurement of surface oxygen groups in Table 2 show that the surface oxygen groups change much by different treatments, and there is an obvious difference in the types of acidic groups. AC-Z has the highest contents of carboxylic, lactones and acidic groups and almost equivalent contents of basic groups as AC-N. AC-H and AC-N contain more phenolic groups (especially AC-H) than the other two samples. However, the carboxylic groups and lactones are undetectable in AC-H.

2.3 Relationship between nicotine adsorption capacity and microporous structure

Micropore is favorable for physical adsorption. Figure 4 represents the nicotine adsorption capacities of the four samples at 308 and 318 K. The samples containing more micropores have higher adsorption performance, even though AC and AC-Z have larger surface areas than AC-H, which is in good agreement with other reports [17,18]. Plots of the nicotine adsorption capacities of samples at different initial concentrations and 308 K versus v_{micro} are shown in Figure 5. The plots in other conditions have the same features (not shown). Linear relationships at 500, 600 and 750 mg/L were obtained with correlation of 0.77, 0.80 and 0.87, respectively, indicating that microporous structure can enhance the nicotine adsorption capacity at high concentrations. There is no linear relationship between nicotine adsorption capacities with low initial concentrations. This may be because micropores and activated sites were abundant for nicotine adsorption at low concentrations, and chemical adsorption also contributes to nicotine adsorption capacity, so the data of adsorbed amounts of nicotine were underrepresented in the conditions.

Table 2 Concentrations of surface oxygen groups of activated carbons

Sample	Carboxylic groups (mmol/g)	Lactones (mmol/g)	Phenolic groups (mmol/g)	Acidic groups (mmol/g)	Basic groups (mmol/g)
AC	0.1912	0.0155	0.0073	0.2140	0.9337
AC-H	–	–	0.1497	0.1497	0.8861
AC-Z	0.2174	0.0481	0.0541	0.3428	0.3196
AC-N	0.1063	0.0343	0.1086	0.2492	0.3466

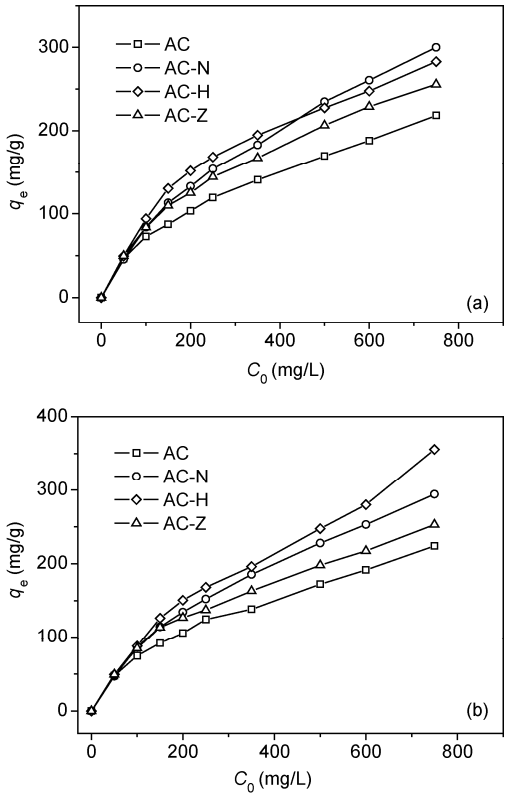

Figure 4 The adsorbed amounts on adsorbents at different initial concentrations at 308 K (a) and 318 K (b).

2.4 Relationship between nicotine adsorption capacity and acidic groups

Surface oxygen groups can obviously affect the adsorption capacity of activated carbon in liquid-phase. The surface oxygen groups of activated carbon often consist of acidic groups (carboxylic groups, phenolic groups, lactone group and carbonyl group) and basic groups, and the acidic groups can act as cations. Generally, the mechanism of nicotine adsorption can be expressed as [3]:

$$\text{Solid-H+R-NH}_2 \leftrightarrow [\text{Solid}^-][\text{NH}_3^+\text{-R}].$$

However, the influences of these acidic groups on the nicotine adsorption capacity are still not found.

The surface group data show that AC and AC-Z contain the highest amounts of carboxylic groups while their nicotine adsorption capacities are lower. On the other hand, AC-H has the similar micropore size distribution as AC-Z except a higher v_{micro}/v_T ratio of 14%, but the adsorbed amount of nicotine of AC-H is much larger. Therefore, it is can be deduced that acidic groups play an important role in

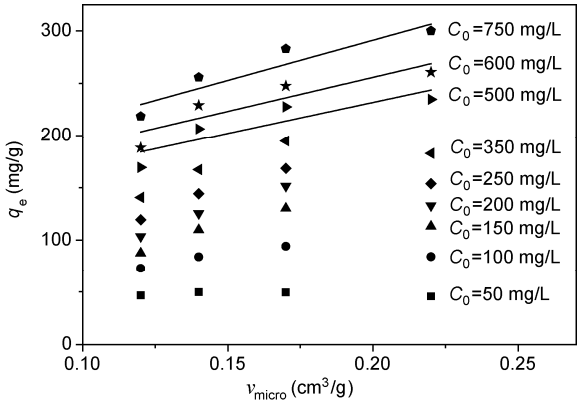

Figure 5 Plots of the nicotine adsorption capacities of adsorbents at different initial concentrations and 308 K versus v_{micro}.

nicotine adsorption, because AC-H has much more phenolic groups. Despite the almost same amount of acidic groups, AC has a much lower nicotine adsorption capacity than AC-N. Comparison of these acidic groups among the four samples shows that AC-H and AC-N have the largest amounts of phenolic groups but lower amounts of carboxylic groups, suggesting that phenolic groups are more effective in increasing the capacitance of activated carbons. In order to analyze the relationship between the nicotine adsorption capacity and phenolic groups, the nicotine adsorption capacity of the four samples are plotted as a function of the contents of phenolic groups. It can be observed that the nicotine adsorption capacities of samples at different initial concentrations and 318 K are proportional to the amount of phenolic groups (Figure 6 (a)), and the plots show high linear relations. The correlation coefficients at 100, 150, 200, 250, 350, 500, 600 and 750 mg/L are 0.70, 0.79, 0.94, 0.99, 0.97, 0.99, 0.99 and 0.94, respectively. Furthermore, Figure 6(b) shows the nicotine adsorption capacities of samples at different initial concentrations and 318 K versus the amount of carboxylic groups. Linear relationships were obtained with correlation of 0.69, 0.85, 0.70, 0.79, 0.84 and 0.90 at 200, 250, 350, 500, 600 and 750 mg/L, respectively. It indicates that nicotine adsorption capacity is inversely proportional to the amount of carboxylic groups, and the influence

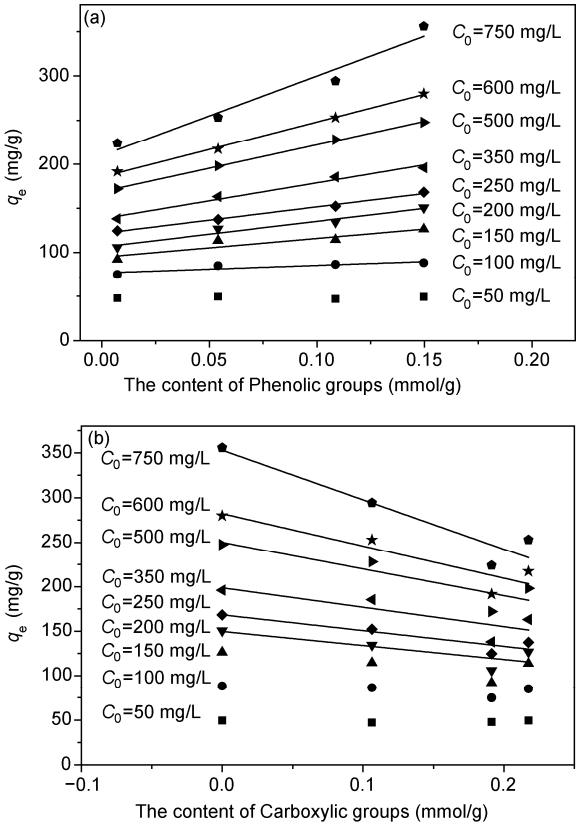

Figure 6 Plots of the nicotine adsorption capacities of adsorbents at different initial concentrations and 318 K versus the content of (a) phenolic groups and (b) carboxylic groups.

was more obvious at high concentrations. The carboxylic groups are responsible for low uptake of nicotine due to its hydration, which blocks the micropores of samples. Moreover, carboxylic groups on the carbon surface act as electron acceptors and remove the π-electron from carbon's basal planes. This may lead to a lower strength of interaction, which decreases the uptake of nicotine. Similar results were already reported [19–21].

3 Conclusions

The influences of microstructure and surface chemistry on the nicotine adsorption capacity of activated carbons are investigated by using different reaction/modification methods for almond-shell-based activated carbon to change the microstructure and surface oxygen groups. The results indicate that adsorption of nicotine from solution onto carbons depends on the micropores, but importantly, on the surface chemistry of the carbons. Phenolic groups can enhance the nicotine adsorption capacity and the amount of phenolic groups is proportional to the nicotine adsorption capacity, whereas nicotine adsorption capacity decreases with an increase amount of carboxylic groups. This decrease is a combined action of two factors. Firstly, the carboxylic groups could combine with water molecules by hydrogen bonds due to its hydration and may block the micropores of activated carbons. Secondly, carboxylic groups on the carbon surface act as electron acceptors and remove the π-electron from carbon's basal planes. This may lead to a lower strength of interaction, which decreases the uptake of nicotine.

This work was supported by the Doctorate Fellowship Foundation of Nanjing Forestry University (2011YB005), China Forestry Science & Technology Promotion Program (2010-34), Industrialization Program of Scientific Achievements in Colleges (JHB2011-11) and National Basic Research Program of China (2010CB732205).

1 Lipowicz P J, Piadé J J. Evaporation and subsequent deposition of nicotine from minstream cigarette smoke in a denuder tube. J Aerosol Sci, 2004, 435: 33–45
2 Chen Z, Zhang L, Tang Y, et al. Adsorption of nicotine and tar from the mainstream smoke of cigarettes by oxidized carbon nanotubes. Appl Surf Sci, 2006, 252: 2933–2937
3 Rakić V, Damjanović L, Rac V, et al. The adsorption of nicotine from aqueous solution on different zeolite structure. Water Res, 2010, 44: 2047–2057
4 Lazarevic N, Adnadjevic B, Jovanovic J. Adsorption of nicotine from aqueous solution onto hydrophobic zeolite type USY. Appl Surf Sci, 2011, 257: 8017–8023
5 Yang J L, Zhou J B. Adsorption of nicotine from aqueous solution by activated carbons prepared from Chinese fir sawdust. Acta Phys Chim Sin, 2013, 29: 377–384
6 Demiral H, Demiral İ, Karabacakoğlu B, et al. Production of activated carbon from olive bagasse by physical activation. Chem Eng Res Des, 2011, 89: 206–213
7 Nowicki P, Wachowska H, Pietrzak R. Active carbons prepared by chemical activation of plum stones and their application in removal

of NO_2. J Hazardous Mater, 2010, 181: 1088–1094
8 Yang H, Yan R, Chen H, et al. Characteristics of hemicellulose, cellulose and lignin pyrolysis. Fuel, 2007, 86: 1781–1788
9 Arami-Niya A, Daud W M A W, Mjalli F S. Comparative study of the textural characteristics of oil palm shell activated carbon produced by chemical and physical activation for methane adsorption. Chem Eng Res Des, 2011, 89: 657–664
10 Mourão P A M, Laginhas C, Custódio F, et al. Influence of oxidation process on the adsorption capacity of activated carbons from lignocellulosic precursors. Fuel Process Technol, 2011, 92: 241–246
11 Shangguan J, Li C, Miao M, et al. Surface characterization and SO_2 removal activity of activated semi-coke with heat treatment. New Carbon Mater, 2008, 23: 37–43
12 Wang H, Kang J, Liu H, et al. Preparation of organically functionalized silica gel as adsorbent for copper ion adsorption. J Environ Sci, 2009, 21: 1473–1479
13 Hanafiah M A K M, Ngah W S W, Zolkafly S H, et al. Acid Blue 25 adsorption on base treated *Shorea dasyphylla* sawdust: Kinetic, isotherm, thermodynamic and spectroscopic analysis. J Environ Sci, 2012, 24: 261–268
14 Dandekar A, Baker R T K, Vannice M A. Characterization of activated carbon, graphitized carbon fibers and synthetic diamond power using TPD and DRIFTS. Carbon, 1998, 36: 1821–1831
15 Ishizaki C, Marti I. Surface oxide structures on a commercial activated carbon. Carbon, 1981, 19: 409–412
16 Wang C P, Wang B L, Liu J T, et al. Adsorption of Cd(II) from acidic aqueous solutions by tourmaline as a novel material. Chin Sci Bull, 2012, 57: 3218–3225
17 Su W, Zhou Y, Wei L, et al. Effect of microstructure and surface modification on the hydrogen adsorption capacity of active carbons. New Carbon Mater, 2007, 22: 135–140
18 Skodras G, Diamantopoulou I, Sakellaropoulos G P. Role of activated carbon structural properties and surface chemistry in mercury adsorption. Desalination, 2007, 210: 281–286
19 Salame I I, Bandosz T J. Role of surface chemistry in adsorption of phenol on activated carbon. J Colloid Interf Sci, 2003, 264: 307–312
20 Figueiredo J L, Mahata N, Pereira M F R, et al. Adsorption of phenol on supercritically activated carbon fibres: Effect of texture and surface chemistry. J Colloid Interf Sci, 2011, 357: 210–214
21 Daifullah A A M, Girgis B S. Impact of surface characteristics of activated carbon on adsorption of BTEX. Colloid Surf A: Physicochem Eng Aspects, 2003, 214: 181–193